DMD Fast Forward. Published on February 16, 2012 as doi: 10.1124/dmd.111.042994

Title of Article:

Mechanistic pharmacokinetic modeling for the prediction of transporter-mediated disposition in human from sandwich culture human hepatocyte data

Author's names:

Hannah M Jones, Hugh A Barton, Yurong Lai, Yi-an Bi, Emi Kimoto, Sarah Kempshall, Sonya C Tate, Ayman El-Kattan, J Brian Houston, Aleksandra Galetin and Katherine S Fenner

Author's affiliations:

Pfizer Worldwide R&D, Department of Pharmacokinetics, Dynamics and Metabolism, Sandwich, Kent, UK (H.M.J., S.K., K.S.F); Pfizer Worldwide R&D, Department of Pharmacokinetics, Dynamics and Metabolism, Groton, Connecticut, US (H.B., Y.L., Y.B., E.K., A.E-K.); Centre for Applied Pharmacokinetic Research, School of Pharmacy and Pharmaceutical Sciences, University of Manchester, Manchester, UK (S.C.T., J.B.H., A.G.).

Running title: Prediction of transporter- mediated disposition in human

Corresponding author:

Hannah M Jones

Current address: Pfizer Worldwide R&D, Department of Pharmacokinetics, Dynamics and Metabolism, 35 Cambridgepark Drive, Cambridge, MA, 02140, U.S.

hannah.jones@pfizer.com

Tel no. +1 617 665 7169

Number of text pages: 22;

Number of tables: 4;

Number of figures: 5;

Number of references: 39;

Number of words in the Abstract: 245;

Number of words in the Introduction: 746;

Number of words in the Discussion: 1491.

DMD Fast Forward. Published on February 16, 2012 as DOI: 10.1124/dmd.111.042994
This article has not been copyedited and formatted. The final version may differ from this version.

Abbreviations:

A, arterial; Abile, amount in bile; Acell, amount in cell; ADME, absorption, distribution, metabolism and excretion; Amedia, amount in media; BDDCS, biopharmaceutics drug disposition classification system; B:P, blood to plasma ratio; C, concentration; cell,u, cell x fu,cell; CEC, extracellular concentration; CIC, intracellular concentration; CL, clearance; CLint, intrinsic clearance; CLint,u,pass, unbound passive diffusion CLint; CLint,u,act, unbound active uptake CLint; CLint,u,bile, unbound bilary CLint; CLint,u,met, unbound metabolic CLint; CLint,u,renal, unbound renal CLint; Cm,tissue, concentration of albumin in liver relative to plasma; CYP450, cytochrome P450; fu,cell, fraction unbound in hepatocyte; fu,media, fraction unbound in the media; fu,p, fraction unbound in plasma; gu, gut; ha = hepatic artery; HLM, human liver microsomes; i.v., intravenous; Kp, tissue to plasma partition coefficient; NME, new molecular entity; KAMC, CLint,u,act/Vm; KMET, CLint,u,met/Vc; KBIL, CLint,u,bile/Vc; KPCM, CLint,u,pass/Vc; KPMC, CLint,u,pass/Vm; li, liver; media,u, media x fu,media; OATP, organic anion transporting polypeptides; PBPK, physiologically based PK; PK, pharmacokinetics; Q, blood flow; SCHH, sandwich culture human hepatocytes; SCLint,u,act, scaled unbound active uptake CLint; SCLint,u,bile, scaled unbound bilary CLint; SCLint,u,met scaled unbound metabolic CLint; SCLint,u,pass, scaled unbound distributional CLint; SD, standard deviation; sp, spleen; T, tissues; u, unbound; V, volume; v, venous; Vc, cell volume; VEC, volume of extracellular compartment; VIC, volume of intracellular compartment; Vinc, volume of the whole incubation; Vm, media volume; Vss, volume of distribution at steady state.

DMD Fast Forward. Published on February 16, 2012 as DOI: 10.1124/dmd.111.042994
This article has not been copyedited and formatted. The final version may differ from this version.

Abstract

With efforts to reduce CYP450-mediated clearance (CL) during the early stages of drug discovery, transporter-mediated CL mechanisms are becoming more prevalent. However, the prediction of plasma concentration-time profiles for such compounds using physiologically based pharmacokinetic (PBPK) modeling is far less established in comparison to compounds with passively mediated PK. In this study, we have assessed the predictability of human PK for seven organic anion transporting polypeptides (OATP) substrates (pravastatin, cerivastatin, bosentan, fluvastatin, rosuvastatin, valsartan and repaglinide) where clinical intravenous (i.v.) data were available. *In vitro* data generated from the sandwich culture human hepatocyte (SCHH) system were simultaneously fit to estimate parameters describing both uptake and biliary efflux. Use of scaled active uptake, passive distribution and biliary efflux parameters as inputs into a PBPK model resulted in the over-prediction of exposure for all seven drugs investigated, with the exception of pravastatin. Therefore, fitting of *in vivo* data for each individual drug in the dataset was performed to establish empirical scaling factors to accurately capture their plasma concentration-time profiles. Overall, active uptake and biliary efflux were under- and over-predicted, leading to average empirical scaling factors of 58 and 0.061, respectively; passive diffusion required no scaling factor. This study illustrates the mechanistic and model-driven application of *in vitro* uptake and efflux data for human PK prediction for OATP substrates. A particular advantage is the ability to capture the multiphasic plasma concentration-time profiles for such compounds using only pre-clinical data. A prediction strategy for novel OATP substrates is discussed.

DMD Fast Forward. Published on February 16, 2012 as DOI: 10.1124/dmd.111.042994
This article has not been copyedited and formatted. The final version may differ from this version.

Introduction

The prediction of human pharmacokinetics (PK) is pivotal to aid in the selection of new molecular entities (NMEs) with appropriate PK properties for clinical development. Physiologically based PK (PBPK) models have long provided a mechanistic framework for improved understanding and predictions of in vivo PK (Bischoff, 1975; Kawai et al., 1998). Successful predictions of human PK have been demonstrated using relevant *in vitro* and physicochemical data within such models (Jones et al., 2006; De Buck et al., 2007; Rostami-Hodjegan and Tucker, 2007; Jones et al., 2011). This approach has proven particularly successful for highly permeable compounds where metabolism is the predominant clearance (CL) mechanism, with negligible contribution of transporters to the overall disposition of these molecules (biopharmaceutics drug disposition classification system (BDDCS) classes 1 and 2, (Wu and Benet, 2005)). It should be emphasized that for these types of compounds, at equilibrium, the intracellular free drug concentration is expected to be equal to the free plasma concentration in the absence of CL from the tissue; therefore, the key PBPK model assumptions of flow mediated distribution and well stirred kinetics are valid. With efforts to reduce CYP450-mediated CL during drug discovery by reducing lipophilicity and increasing polarity, transporter-mediated PK is becoming more prevalent, particularly as the focus of drug discovery is moving away from the typical aminergic G-protein coupled receptors and enzyme targets to ion channels and peptidic receptors. For these more poorly permeable compounds (BDDCS classes 3 and 4, (Wu and Benet, 2005)) liver transporters may become an important determinant of disposition. The use of generic PBPK models therefore becomes limited, as hepatic uptake will lead to significant differences between the free concentrations in the hepatocyte and plasma.

A number of recent studies provide evidence that compounds with poorly predicted PK are often substrates for transporters (Soars et al., 2009; Watanabe et al., 2010). Improvement in PK prediction for such compounds requires accurate estimation of the

extent of active uptake and/or efflux in the hepatocyte. The movement of a compound across the hepatocyte cell membrane is modulated via passive diffusion and active transport, such as active uptake via organic anion transporting polypeptides (OATP). Once in the hepatocyte, substrates may be metabolized via CYP450-mediated metabolism or excreted into the bile via efflux transporters, e.g., multidrug resistance protein 2 or breast cancer resistance protein. This has resulted in the development of a number of *in vitro* assays with varying complexity that allow assessment of these processes either in isolation or combination (Giacomini et al., 2010). These include suspended hepatocytes (Kitamura et al., 2008; Paine et al., 2008), plated hepatocytes (Poirier et al., 2008; Yabe et al., 2011), sandwich cultured hepatocytes (Lee et al., 2010; Yan et al., 2011) and a range of transfected cell lines expressing individual transporters (Yamashiro et al., 2006; Kitamura et al., 2008).

The sandwich cultured human hepatocyte system (SCHH) involves culturing hepatocytes in a sandwich format between collagen and matrigel to allow polarisation of the cells (Liu et al., 1999; Bi et al., 2006; Lee et al., 2010). Through modulation of calcium ions, this *in vitro* system can be used to assess both uptake and biliary efflux (Liu et al., 1999; Bi et al., 2006). Simultaneous assessment of all the processes occurring in SCHH and mechanistic application of the data generated is currently lacking.

Mechanistic models have been used to describe *in vitro* uptake in suspended and plated hepatocytes (Paine et al., 2008; Poirier et al., 2008). Such *in vitro* data have been integrated either into semi-mechanistic or whole body PBPK models to simulate *in vivo* PK for OATP substrates in rat (Paine et al., 2008; Poirier et al., 2009a; Poirier et al., 2009b; Watanabe et al., 2009) and human (Poirier et al., 2009a; Watanabe et al., 2009). In most cases, successful predictions were only achieved when empirical scaling factors were incorporated.

The aim of this work was to examine the predictability of transporter mediated PK in humans using seven OATP substrates, selected based on the availability of clinical intravenous (i.v.) data. The SCHH assay was optimized to allow investigation of active/passive uptake and biliary efflux in the same hepatocyte donor and under the same experimental conditions. For each compound, *in vitro* SCHH data were simultaneously modeled to generate *in vitro* parameter estimates. In conjunction with other ADME and physicochemical properties, these parameters were then incorporated into a whole body PBPK model to assess the predictability of the clinical PK. A scaling approach is proposed and its potential application to novel compounds is discussed.

DMD Fast Forward. Published on February 16, 2012 as DOI: 10.1124/dmd.111.042994
This article has not been copyedited and formatted. The final version may differ from this version.

Materials and Methods

Materials. Compounds were purchased from Sequoia Research Products (Pangbourne UK), HT media, CP media, HI media and torpedo antibiotic mix were purchased from Celsis IVT (Baltimore, MD, USA), matrigel was purchased from BD BioSciences (Woburn, MA, USA), HBSS (Hanks balanced salt solution) was purchased from Invitrogen (Carlsbad, CA, USA) and all other chemicals were purchased from Sigma-Aldrich (St Louis, MO, USA).

Compound selection. Seven compounds were investigated, namely pravastatin, cerivastatin, bosentan, fluvastatin, rosuvastatin, valsartan and repaglinide. Compound selection was based on the availability of clinical i.v. data. Corresponding *in vitro* and physicochemical data were generated in house for these compounds using standard assays that have been described elsewhere in the literature (Allan et al., 2008).

Sandwich culture human hepatocyte (SCHH) experimental procedure. Cryopreserved human hepatocytes from donors HU4168, RTM and BD109 were purchased from CellzDirect (Pittsboro, NC, USA), Celsis IVT (Baltimore, MD, USA) and BD BioSciences (Woburn, MA, USA) respectively. These lots have been previously characterized in house and are known to have functional transport activity. The hepatocytes were cultured in a sandwich format as reported previously (Bi et al., 2006; Li et al., 2010).

Briefly, the cryopreserved hepatocytes were thawed in completed HT medium (thawing medium) and spun down at 50 xg for 3 minutes. The excess medium was removed and the hepatocyte pellet was re-suspended to 7.0 x 10^5 cells mL in completed CP medium (plating medium). The hepatocyte suspension was then seeded onto 24-well BioCoat collagen I plates at 0.5 mL per well and cells allowed to attach overnight in a humidified incubator at 37 °C with 5% CO2. On day 2, the excess hepatocytes were removed and the wells were washed with completed HI culture medium (incubation medium) at room temperature. Each well was then overlaid with BD Matrigel™ at a concentration of 0.25 mg/mL in ice-cold

DMD Fast Forward. Published on February 16, 2012 as DOI: 10.1124/dmd.111.042994
This article has not been copyedited and formatted. The final version may differ from this version.

completed HI medium. Media were replaced with completed HI medium daily until the day of the experiment.

On day 5, cells were washed twice and pre-incubated for 10 minutes at 37 °C in either: (a) HBSS buffer containing 0.1 mM rifamycin SV (inhibits a range of transporters (Vavricka et al., 2002)), (b) HBSS buffer or (c) Ca^{2+}/Mg^{2+} free HBSS containing 1 mM EGTA. Incubations were performed in 2 donors (except bosentan) and on a number of occasions. Substrates dissolved in the relevant condition buffer were added at 1 or 2 µM and incubated at 37 °C over 0.5-30 minutes; a minimum of 3 time points were taken in duplicate for each condition. Rosuvastatin was used as a positive control in all experiments. The cells were lysed with 0.5 mL methanol containing internal standard at room temperature for 20 minutes at 150 rpm. The samples were transferred to a 96 deep well plate and evaporated under 40 °C gaseous N2. The residue was reconstituted in 70% methanol and analysed using LC-MS/MS. Parallel wells of hepatocytes were lysed with RIPA buffer (TEKnova) or M-PER Mammalian Protein Extraction Reagent (Thermo Scientific (Waltham, MA)) for protein quantification by BCA Protein Assay Kit - Reducing Agent Compatible (Thermo Scientific (Waltham, MA)). Protein amounts were determined from the difference between the protein amount for each hepatocyte donor and the protein amount in blank wells, containing Matrigel™ alone.

Bioanalysis procedure. Analysis of 20 µL samples was carried out using HPLC (Hewlett Packard G1310 1100 Series Isocratic Pump) followed by MS/MS (MDS Sciex API 4000) using a 2 minute run time per sample. The mobile phase used to load the column (Dash HTS Hypersil Gold 20x2.1mm 5µm) was 2mM ammonium acetate in 90% methanol containing 0.027% formic acid (v/v); elution was performed at 0.7 min using a mobile phase of 2mM ammonium acetate in 10% methanol containing 0.027% formic acid (v/v). The flow rate was set at 1 mL/min. The mass:charge ratio (m/z) and collision energies (eV) for each compound were: pravastatin m/z 423→101 -40eV, cerivastatin m/z 460→356 50eV, bosentan m/z 552→202 40eV, fluvastatin m/z 412→266 1.11 25eV, rosuvastatin m/z 480→418 -25eV,

DMD Fast Forward. Published on February 16, 2012 as DOI: 10.1124/dmd.111.042994
This article has not been copyedited and formatted. The final version may differ from this version.

valsartan m/z 434→350 -25eV, repaglinide m/z 453→230 25eV. The internal standard used in all analyses was an in house compound (PF-05218881: m/z 688→366 negative ion mode, m/z 686→366 positive ion mode).

***In vitro* data analysis.** The modeling approach used to analyse the SCHH data was analogous to the method described previously for suspended and plated hepatocytes by Paine and Poirier respectively (Paine et al., 2008; Poirier et al., 2008). To address biliary excretion, additional model terms have been proposed for the analysis of extended incubation times (Lee et al., 2010); however, these parameters cannot be estimated with the duration of experiment used here.

The model includes compartments representing the media, cell and bile environments of the experiment, with passive diffusion, active uptake and efflux processes incorporated in a mechanistic fashion, as illustrated in Figure 2. The passive diffusion component was parameterized as an unbound distribution CL (CLint,u,pass) within the model. Active uptake was parameterized in the form of an unbound uptake CL (CLint,u,act). Two further clearance mechanisms were incorporated, namely unbound biliary CL (CLint,u,bile) and unbound metabolic CL (CLint,u,met). Efflux transport by sinusoidal transporters was assumed negligible. There are studies to suggest bidirectional transport by OATPs, but these are generally based on oocyte data (Mahagita et al., 2007) and have not been considered here. It was assumed that only unbound drug is able to pass across the cell membrane, and that any binding to the cell membrane is instantaneous. The equations used in this modeling process are shown below.

$$\frac{dAmedia}{dt} = -KPMC \cdot Amedia,u + KPCM \cdot Acell,u - KAMC \cdot Amedia,u + KBIL \cdot Acell,u \quad (1)$$

$$\frac{dAcell}{dt} = KPMC \cdot Amedia,u - KPCM \cdot Acell,u + KAMC \cdot Amedia,u - KBIL \cdot Acell,u - KMET \cdot Acell,u \quad (2)$$

DMD Fast Forward. Published on February 16, 2012 as DOI: 10.1124/dmd.111.042994
This article has not been copyedited and formatted. The final version may differ from this version.

$$\frac{dAbile}{dt} = KBIL \cdot Acell,u \quad (3)$$

where KPMC = CLint,u,pass/Vm; Vm = media volume (µL); u = unbound; KPCM = CLint,u,pass/Vc; Vc = cell volume (µL); KAMC = CLint,u,act/Vm; KMET = CLint,u,met/Vc; KBIL = CLint,u,bile/Vc; Amedia = amount in media (pmoles); Acell = amount in cell (pmoles); Abile = amount in bile (pmoles); cell,u = cell x fu,cell; media,u = media x fu,media.

CLint units were µL/min/Mcells and it was assumed based on in-house data that 1 Mcells = 1 mg protein. The volume of the whole incubation (Vinc) is the sum of the medium and cell volumes, Vm and Vc, respectively. Vc was estimated assuming 1 Mcells is equivalent to 4 µL (Reinoso et al., 2001). The fraction unbound in the media (fu,media) was assumed to equal 1, as no protein was present. The fraction unbound in the hepatocyte (fu,cell) was calculated using a rearranged form of the equation reported by (Poulin and Theil, 2000), assuming the concentration of albumin in liver relative to plasma (Cm,tissue) is equal to 0.5. This parameter accounts for non-specific binding of the drug intracellularly within the hepatocyte and was fixed in further modeling of *in vitro* data.

$$fu,cell = \frac{1}{1 + \left(\frac{1 - fu,p}{fu,p} \cdot Cm,tissue \right)} \quad (4)$$

where fu,p is the fraction unbound in the plasma.

Nonzero initial conditions were set for the cell and media compartments to account for instantaneous nonspecific binding to cells and/or experimental apparatus. This amount was calculated from Vm, Vc and the binding constant (KB) as described in the literature (Paine et al., 2008; Poirier et al., 2008)(Equations 5 and 6).

$$Amedia(t=0) = Amedia - \frac{Amedia}{Vm} \cdot KB \cdot Vc \quad (5)$$

DMD Fast Forward. Published on February 16, 2012 as DOI: 10.1124/dmd.111.042994
This article has not been copyedited and formatted. The final version may differ from this version.

$$Acell(t=0) = \frac{Amedia}{Vm} \cdot KB \cdot Vc \quad (6)$$

Where significant metabolism was observed, CLint,u,met was set to the unbound CLint value determined in human liver microsomes (HLM), adjusted from µL/min/mg to µL/min/Mcells using the ratio of hepatocellularity to microsomal recovery (HLM CLint,u x microsomal recovery / hepatocellularity). The model fitting of CLint,u,pass, CLint,u,act, CLint,u,bile and KB was performed in NONMEM version VI level 1.2., NM-TRAN subroutines version III level 1.2 (Icon Development Solutions, Ellicott City, Maryland, USA, 2006) or in acslX version 3.0.1.6 (Aegis Technologies, Huntsville, AL, USA). The HYBRID estimation method in NONMEM was employed, where first-order estimation (FO) was used to estimate all the parameters. Residual error was estimated using a proportional error model.

***In vivo* simulations.** An i.v. PBPK model was used to model the *in vivo* situation. The PBPK model was composed of 15 compartments corresponding to the different tissues of the body, namely, adipose, bone, brain, gut, heart, kidney, liver, lung, muscle, skin, spleen, testes, rest of body which were connected by the circulating blood system (arterial and venous). Each compartment was defined by a tissue volume and a tissue blood flow rate; these physiological parameters for human have been described elsewhere (Jones et al., 2006). Each tissue was assumed to be perfusion rate limited, with the exception of liver. The liver and kidney were considered to be the only sites of elimination.

The mass balance differential equations (except for liver) used in the model have been described previously (Jones et al., 2006; Jones et al., 2011) and follow the principles shown below.

$$\text{non-eliminating tissues: } VT \cdot \frac{dCT}{dt} = QT \cdot Ca - QT \cdot CvT \quad (7)$$

DMD Fast Forward. Published on February 16, 2012 as DOI: 10.1124/dmd.111.042994
This article has not been copyedited and formatted. The final version may differ from this version.

where Q = blood flow (L/hr); C = concentration (mg/L); V = volume (L); T = tissues; a = arterial; v = venous; CvT = CT/Kp*B:P; Kp = tissue to plasma partition coefficient of the compound; B:P = blood to plasma ratio.

$$\text{kidney: } VT \cdot \frac{dCT}{dt} = QT \cdot Ca - QT \cdot CvT - CLint,u,renal \cdot CvT,u \quad (8)$$

where CLint,u,renal = the unbound renal intrinsic clearance of the compound (L/hr).

CLint,u,renal was calculated from the renal CL reported from the respective clinical study assuming well stirred conditions (Supplementary Material, Table S1).

The Kp values (for all tissues except for the liver) were estimated using tissue composition equations developed in the literature (Rodgers and Rowland, 2006). The tissue composition parameters reported by the authors were used. The main compound specific parameters required were $LogD_{7.4}$, pKa, B:P ratio and fu,p. These predictive equations account for four main processes: (1) partitioning of unionized drug into neutral lipids and neutral phospholipids, (2) dissolution of ionized and unionized drug in tissue water (3) electrostatic interactions between ionized drug and acidic phospholipids for strong ionized bases and (4) interactions with extracellular protein for neutrals, weak bases and acids. These equations assume only passive distribution and do not account for any active transport processes. Tissue composition data and anatomical information were available for each tissue in the model. It was desirable to include the full PBPK model to get initial estimates of exposure related to safety concerns and to provide a framework for elaboration of transporters in other tissues.

The liver was modeled as a permeability-limited tissue, incorporating scaled active uptake (SCLint,u,act) and scaled passive diffusion clearances (SCLint,u,pass) of unbound drug at the sinusoidal membrane, scaled biliary clearance (SCLint,u,bile) of unbound drug at the canalicular membrane and scaled metabolic clearance (SCLint,u,met) of unbound drug

(where appropriate). These scaled parameters (L/h) were calculated from the *in vitro* parameters CLint,u,act, CLint,u,pass, CLint,u,bile and CLint,u,met obtained in SCHH, accounting for the hepatocellularity and liver weight as described previously (Houston, 1994). The liver compartment was sub-divided into five units of extracellular and intracellular compartments, connected by blood flow in tandem (Watanabe et al., 2009), as shown in Figure 2. Watanabe and coworkers reported that for pravastatin, five sequential compartments most closely approximated the partial differential equation dispersion model, so this number of compartments was retained. Initial modeling (results not shown) used one liver tissue and liver blood. The corresponding differential equations used are shown below:

Extracellular liver 1:

$$\frac{VEC}{5}\cdot\frac{dCEC_1}{dt} = Qha\cdot Ca + Qgu\cdot Cvgu + Qsp\cdot Cvsp - Qli\cdot CEC_1 - \frac{SCLint,u,pass}{5}\cdot\left(CEC_1u - CIC_1u\right) - \frac{SCLint,u,act}{5}\cdot CEC_1u \quad (9)$$

where CEC = extracellular concentration (mg/L); CIC = intracellular concentration (mg/L); VEC = volume of extracellular compartment (L); VIC = volume of intracellular compartment (L); ha = hepatic artery; gu = gut; sp = spleen; li = liver.

Extracellular liver 2-5:

$$\frac{VEC}{5}\cdot\frac{dCEC_i}{dt} = Qli\cdot\left(CEC_{i-1} - CEC_i\right) - \frac{SCLint,u,pass}{5}\cdot\left(CEC_iu - CIC_iu\right) - \frac{SCLint,u,act}{5}\cdot CEC_iu \quad (10)$$

Intracellular liver 1-5:

$$\frac{VIC}{5}\cdot\frac{dCIC_i}{dt} = \frac{SCLint,u,pass}{5}\cdot\left(CEC_iu - CIC_iu\right) + \frac{SCLint,u,act}{5}\cdot CEC_iu - \frac{SCLint,u,bile}{5}\cdot CIC_iu - \frac{SCLint,u,met}{5}\cdot CIC_iu \quad (11)$$

DMD Fast Forward. Published on February 16, 2012 as DOI: 10.1124/dmd.111.042994
This article has not been copyedited and formatted. The final version may differ from this version.

The model simulations were performed in Berkeley Madonna, version 8.3.9 (University of California, USA, 1996-2006).

Maximal contribution of the active process to the total uptake was estimated and expressed as the ratio of CLint,u,act and total uptake CLint (CLint,u,act + CLint,u,pass).

***In vivo* fitting.** In addition to the simulations, a fitting procedure was performed. Using the observed clinical i.v. data (extracted via DigitizeIt version 1.5.7), the SCLint,u,act, SCLint,u,pass and SCLint,u,bile were estimated by the PBPK model assuming that all other parameters within the model were correct and using the scaled parameter values as the initial estimates. For cerivastatin, bosentan and fluvastatin where metabolic and biliary clearance data were available, the sum of SCLint,u,bile and SCLint,u,met were fitted as SCLint,u,bile could not be uniquely identified. For repaglinide, SCLint,u,bile was assumed negligible and the predicted SCLint,u,met was fixed. The fitting procedure was performed using a proportional error model implemented within Berkeley Madonna by log transformation of the data. For the individual compounds, empirical scaling factors were calculated for each of these parameters by dividing the measured (scaled to intact liver) value by the fitted value.

The geometric mean of the empirical scaling factors across the drugs in the dataset was calculated. The i.v. PK for each compound was further simulated using the *in vitro* data together with the average empirical scaling factors within the PBPK model. The simulations were compared graphically with the observed clinical data. The predicted PK profiles with and without average empirical scaling factors were modeled in WinNonlin version 5.2 (Mountain View, CA) using non-compartmental analysis to determine volume of distribution at steady state (Vss) and CL parameters.

Local sensitivity analyses: Local sensitivity analyses were conducted in acslX version 3.0.1.6 (Aegis Technologies, Huntsville, AL, USA) for each of the seven compounds to obtain

numerical estimates of the partial derivative of the model with respect to each parameter. Each parameter was raised or lowered by 1% with respect to its value for that compound and the value of the plasma concentration was obtained at three selected times throughout the time course during simulations of the conditions used for fitting *in vivo* parameters. Sensitivity coefficients were normalized to both the parameter value and the model output value, so when the output changes by 1% for a 1% change in the input parameters, the sensitivity coefficient is 1 or -1 depending upon the direction of change. Only parameters with normalized sensitivity coefficients greater than 0.3 or less than -0.3 are reported.

DMD Fast Forward. Published on February 16, 2012 as DOI: 10.1124/dmd.111.042994
This article has not been copyedited and formatted. The final version may differ from this version.

Results

Physicochemical properties. A summary of the available *in vitro* data (excluding hepatic uptake data) and physicochemical properties for pravastatin, cerivastatin, bosentan, fluvastatin, rosuvastatin, valsartan and repaglinide is shown in Table 1. All compounds were acidic. The $LogD_{7.4}$ measurements ranged from very hydrophilic at -0.88 for valsartan to lipophillic at 2.1 for repaglinide. B:P ratios were comparable across compounds, ranging from 0.48-0.76. For cerivastatin, bosentan, fluvastatin, valsartan and repaglinide, fu,p values were very low (< 1%), whereas fu,p values for rosuvastatin and pravastatin were higher at 9.4 and 43%, respectively. HLM CLint values were determined via substrate depletion experiments and corrected for nonspecific binding. Pravastatin, rosuvastatin and valsartan had no measurable metabolism in HLM, whereas CLint,u,met ranged from 22-128 µL/min/mg for the remaining compounds (Table 1).

Clinical data. The corresponding human PK parameters for each compound are reported in Table S1 (Supplementary Material). These data were obtained from i.v. PK studies reported in the literature (see References in Supplementary Material). CL ranged from 0.49-14mL/min/kg for valsartan and pravastatin, respectively, whereas Vss covered a 10-fold range with fluvastatin and rosuvastatin at the low and high end, respectively. Pravastatin, rosuvastatin and valsartan exhibited 29-47% contribution of renal excretion to their total CL.

***In vitro* data SCHH analysis.** The in vitro SCHH data obtained for all seven drugs investigated are shown in Figure S1 in the Supplementary material. The SCHH data were simultaneously modeled as described in the methods section and Figure 1. The derived parameter estimates of CLint,u,act, CLint,u,pass, CLint,u,bile are shown in Table 2. This assay was performed in 2 donors (except bosentan) and on a number of occasions. For the purposes of modeling, fu,cell, which describes the free fraction in the cell and the fraction nonspecifically bound (i.e., 1 - fu,cell) was fixed to the value predicted using Equation 4. Within the fitting process,

DMD Fast Forward. Published on February 16, 2012 as DOI: 10.1124/dmd.111.042994
This article has not been copyedited and formatted. The final version may differ from this version.

sinusoidal efflux was assumed to be negligible. The parameter values were estimated to an acceptable precision level and diagnostic plots and visual inspection of the observed versus fitted data indicated a good model fit (plots not shown). A 60-fold range in total uptake CLint values was observed, with pravastatin showing the lowest total uptake CLint (below 2µL/min/Mcells) and repaglinide the highest (119µL/min/Mcells). Despite this, the maximal contribution of active processes to uptake CLint varied and was not necessarily correlated with the total uptake CLint. Pravastatin and valsartan both exhibited low uptake into the hepatocyte; however, the maximal active contribution was proportionally high at 95 and 78%, respectively. In contrast, the total uptake of fluvastatin and repaglinide were much higher, with maximal active contributions of 69 and 25% respectively; for these compounds the contribution of passive diffusion was substantial and also subject to variability in the case of repaglinide. Bosentan, cerivastatin, and rosuvastatin exhibited intermediate uptake with a range of maximal active uptake contribution of 65, 28 and 85% respectively. CLint,u, bile of the parent compound varied for the different compounds from 0 in the case of repaglinide to 96µl/min/Mcells for valsartan. For all these compounds, uptake CLint (passive and active) determined in suspended hepatocytes was within 2-3 fold of the SCHH data (data not shown).

***In vivo* simulations and fitting.** The *in vitro* parameters derived from the simultaneous modeling of the SCHH data and the HLM CLint,u,met were scaled to the *in vivo* situation to account for hepatocellularity, microsomal recovery and liver weight. Scaled SCLint,u,act, SCLint,u,pass, SCLint,u,bile and SCLint,u,met parameters are shown in Table 3 for all the drugs investigated. The Kp values, fu,p, fu,cell and B:P ratio as well as SCLint,u,active, SCLint,u,passive, SCLint,u,bile and SCLint,u,met were input into the whole body PBPK model described in the methods section and Figure 2. The clinical dose was simulated for each compound using the whole body PBPK model. The simulated versus observed profiles for each compound are shown in Figure 3. The simulation overpredicted the exposure when

compared to the observed data, except for pravastatin and rosuvastatin, suggesting underestimation of the initial distribution phase.

To rationalize the misestimation of the observed human i.v. plasma concentration time profile, the SCLint,u,act, SCLint,u,pass and SCLint,u,bile were estimated using the model and the observed clinical i.v. data, assuming that all other parameters within the model were correct. These fitted parameters are shown in Table 3 and the profiles originating from these fitted parameters are shown in Figure 3, in parallel to the initial simulations. As can be seen in Figure 3, the fit for each compound accurately describes the observed plasma concentration-time data and corresponds to the shape of the observed profile. Goodness of fit plots are shown in Figure S2 in the Supplementary material. The fitted parameters were compared to the predicted parameters for each drug to generate an empirical scaling factor. The *in vivo* fitted SCLint,u,act was significantly ($p<0.0001$) higher than the *in vitro* scaled value for the entire dataset, with empirical scaling factors ranging from 12-161 for rosuvastatin and fluvastatin, respectively, resulting in a geometric mean empirical scaling factor of 58. Consistent with expectations for a model approximating the liver acinar gradient (5-sequential subcompartments) versus a single tissue and blood compartment, initial modeling with the single unit model required higher empirical scaling factors for fluvastatin and other compounds with high active uptake. In contrast, values were more comparable between the two models for rosuvastatin and compounds with slower uptake rates, with a geometric mean empirical scaling factor of 95 (results not shown). In the majority of cases the *in vivo* fitted and *in vitro* scaled SCLint,u,pass compared well with each other giving a geometric mean scaling factor of 1. The only exception was valsartan where scaling of passive permeability was required to fit the terminal phase of the profile. For each of the seven compounds, the *in vivo* fitted SCLint,u,bile was on average 16-fold lower than the *in vitro* scaled value, giving empirical scaling factors below 1 (Table 3). For cerivastatin, bosentan and fluvastatin, the empirical scaling factors for SCLint,u,bile could not be

estimated as these compounds also undergo measureable P450 metabolism and the model could not uniquely identify these two parameters. For this reason the two parameters were summed and fitted together. For repaglinide, there was no measurable CLint,u,bile. The empirical scaling factor for SCLint,u,bile (0.061) was therefore calculated using only 3 compounds (pravastatin, rosuvastatin and valsartan).

These average empirical scaling factors for active uptake and biliary efflux were subsequently re-applied to the seven compounds to re-simulate the clinical i.v. data. Figure 4 shows simulated plasma concentration time profiles based on the SCHH estimates for SCLint,u,act, SCLint,u,pass and SCLint,u,bile scaled by the average empirical scaling factors of 58, 1 and 0.061 for the corresponding processes, respectively; all other parameter inputs were as used for simulations shown in Figure 3. Use of average empirical scaling factors, compared to simulations performed without them, resulted in better agreement between the simulated profile and observed data for the majority of the compounds. The biphasic profile for bosentan was not accurately captured using the generic empirical scaling factor; the fitting procedure reduced combined metabolism and biliary efflux to a value lower than SCLint,u,met (55 versus 87 L/hr) (Table 3), whereas for the re-simulation the *in vitro* metabolism scaled value was used.

The predicted Vss and CL parameters using different modeling scenarios are shown in Table 4. For each compound both the CL and Vss were under predicted when the *in vitro* data alone were used in the PBPK model with an absolute average fold error of 7.1 and 3.0 respectively. However, when these data were corrected for the average empirical scaling factors the predicted CL and Vss parameters corresponded more accurately with the observed data with absolute average fold errors of 1.3 and 1.7, respectively.

Local sensitivity analyses: For each of the seven compounds, all parameters were investigated to assess their sensitivity to the model simulation of the plasma concentration

profile. This analysis included all the physiological parameters in the model as well as those specific for each compound. Very few of the physiological parameters had normalized sensitivity coefficients greater than 0.3 or less than -0.3, indicating very limited impact when these parameters were varied individually (data not shown). Physiological parameters to which multiple compounds were sensitive included body weight, cardiac output, volume of liver tissue and liver blood flow. The fu,p, fu,cell, B:P ratio, SCLint,u,act and SCLint,u,pass, were sensitive parameters, along with SCLint,u,bile, SCLint,u,met and CLint,u,renal as appropriate to each compound. The sensitive parameters showed complex changes as would be expected for the different exposure regimens and varying importance of processes throughout the duration of the observed plasma time course. Figure 5, illustrates that the early plasma time course is increasingly sensitive to liver uptake (with SCLint,u,act and SCLint,u,pass having opposite impacts), while the later time course becomes increasingly sensitive to the clearance from the liver (SCLint,u,bile and SCLint,u,met) and CLint,u,renal.

DMD Fast Forward. Published on February 16, 2012 as DOI: 10.1124/dmd.111.042994
This article has not been copyedited and formatted. The final version may differ from this version.

Discussion

Prediction of human PK remains an important feature of drug discovery to help select compounds with appropriate characteristics for clinical development. Physiologically based methods for human PK prediction are reasonably well established for small lipophilic compounds cleared by liver metabolism (Jones et al., 2006; De Buck et al., 2007; Rostami-Hodjegan and Tucker, 2007; Jones et al., 2011) and have recently been applied for better understanding of intestinal first-pass (Gertz et al., 2011). However, the optimization of compound properties to improve metabolic stability has led to a reduction in lipophilicity and permeability and hence a shift in CL routes from liver metabolism to transporter mediated uptake and efflux. The prediction of such processes in humans continues to be a challenge (Liu and Pang, 2006; Poirier et al., 2009a; Watanabe et al., 2009).

Using a SCHH *in vitro* system together with available clinical plasma concentration-time data for seven compounds, we have established a prediction approach for active liver uptake and efflux. These SCHH *in vitro* data were dynamically modeled as outlined in Figure 1. In contrast to previous modeling efforts (Paine et al., 2008; Poirier et al., 2008), the current model allowed estimation of biliary efflux, active and passive uptake from the same *in vitro* experiment through modulation of calcium ions (Liu et al., 1999; Bi et al., 2006; Lee et al., 2010; Yan et al., 2011). The *in vitro* mechanistic model was parameterized in such a way to separate out the intracellular binding and the active processes; hence, the fu,cell term was fixed to the predicted value. An accurate estimation of this parameter is particularly important to estimate the free concentration in the liver and influences the rate of metabolism/biliary excretion. Here fu,cell was predicted using Equation 4, however improved prediction approaches may be needed (Yabe et al., 2011). These *in vitro* parameters were then scaled to *in vivo* and were subsequently integrated into a whole body PBPK model, together with other ADME properties, to simulate the human plasma concentrations (Figure 2). Prediction accuracy of these simulations was assessed by

comparison with observed plasma concentration-time profiles reported in the literature. The simulations in Figure 3 show that the plasma concentration time profiles were significantly over estimated, with the initial phase of the profile being significantly mis-predicted, perhaps indicating an underprediction of the initial distribution into the liver, as observed by others (Poirier et al., 2009a; Watanabe et al., 2009). Using a fitting procedure, the PBPK model together with the observed plasma concentration-time data were used to estimate the *in vivo* values for the SCLint,u,act, SCLint,u,pass and SCLint,u,bile that would better describe the observed data. Table 3 shows the fitted values together with the empirical scaling factors describing the relationship between the fitted and measured parameters. In general SCLint,u,act and SCLint,u,bile were under- (58-fold) and over-predicted (16-fold), respectively; no empirical scaling factor was required for passive diffusion. The values for empirical scaling factors reported here are specific to our implementation of the SCHH; other laboratories would need to re-estimate their own system specific empirical scaling factors.

Previous studies have also reported the need for empirical scaling factors for active uptake for pravastatin and valsartan to recover the human plasma concentrations (Poirier et al., 2009a; Watanabe et al., 2009). The basis for this empirical scaling factor is unclear. An evaluation of OATP expression in SCHH, showed that, while OATP1B3/ OATP2B1 expression were reduced to ~50% of that in suspension, OATP1B1 expression was increased to ~150% (Table S2, Supplementary Materials). These results are consistent with recent studies that show no effect of the culture time on uptake transporter activity in SCHH for rosuvastatin (Kotani et al., 2011), which would not support the hypothesis that the expression of uptake transporters is downregulated in this system. However, the difference between OATP expression in culture and *in vivo* is unknown. The model fitting was performed using plasma concentration-time data alone; the lack of liver concentration data to assist in model fitting may mean that the fitted values for SCLint,u,act, SCLint,u,pass and SCLint,u,bile have not

DMD Fast Forward. Published on February 16, 2012 as DOI: 10.1124/dmd.111.042994
This article has not been copyedited and formatted. The final version may differ from this version.

been estimated accurately, though this would be expected to have more impact on the biliary transport value than the active uptake. However, the issue of parameter identifiability has been investigated and the combination of parameters obtained by fitting appeared unique in their ability to accurately describe the plasma concentration-time profiles of these compounds (see contour plots in Supplemental material, Figure S3) given the model structure used and the values of the other parameters. In addition, the fitting routine assumes that all other parameters within the PBPK model were correct and that all other tissues (excluding the liver) are perfusion rate limited. However, expression of OATP transporters has been reported in other tissues, e.g., kidney (Hilgendorf et al., 2007) and this could partially explain the large empirical scaling factors required when liver alone is assumed to be the main transport organ. Initial data on transporter abundance are becoming available (Schaefer et al., 2011); however, until detailed transporter expression data are reported for the liver and other tissues, this will remain a caveat of this analysis. In terms of the passive uptake into the liver, the SCLint,u,pass scaled accurately from *in vitro* to *in vivo,* probably due to the lack of dependence on an enzymatic or active processes that could be up- or down-regulated on culturing. This has been observed also by others in the literature in human and rat (Paine et al., 2008; Poirier et al., 2009a; Poirier et al., 2009b; Watanabe et al., 2009).

One limitation of the modeling reported here is that it does not address enterohepatic recirculation for the drugs with substantial biliary excretion, as explicitly demonstrated with rosuvastatin in rats (Nezasa et al., 2002). The absence of recycling would mean that the estimated biliary efflux would represent only the net CL (i.e., excreted minus reabsorbed) resulting in the observed overprediction. A more complex model to describe the recycling of drug from bile back into the intestine is required to fully understand this empirical scaling factor and would facilitate incorporation of additional published human data for intraduodenal dosing and biliary excretion of rosuvastatin (Bergman et al., 2006).

DMD Fast Forward. Published on February 16, 2012 as DOI: 10.1124/dmd.111.042994
This article has not been copyedited and formatted. The final version may differ from this version.

An evaluation of our SCHH assay indicated that these biliary efflux proteins are upregulated by ~3-fold during the 5 day culture period, which would also in part explain the overprediction observed (unpublished data).

The sensitivity analysis showed complex changes as would be expected for the different exposure regimens and varying importance of processes throughout the duration of the observed plasma time course, illustrating the value of fitting multiphasic i.v. plasma concentration-time data for estimation of the empirical scaling factors (to estimate misprediction) rather than relying solely on reported PK parameter values.

Although each compound showed the same trend in terms of empirical scaling factors, there was a high degree of variability in the derived values, suggesting that the *de novo* application of these parameters to novel compounds may be uncertain. This variability could result from several factors e.g. multiple/different transporters between compounds and genetic polymorphisms for some transporters. The purpose of this analysis was to explore the utility of using SCHH data to simulate human transporter-mediated PK. Several issues have been identified that require further investigation. Availability of *in vitro* transporter data in a larger number of donors in conjunction with protein expression data is required to further improve transporter IVIVE. However, Figure 4 shows that the application of the average empirical scaling factors to these compounds gives a reasonable description of the plasma concentration-time profile. In addition, the application of these average empirical scaling factors results in a good prediction accuracy for CL and Vss parameters with absolute average fold errors of 1.3 and 1.7 respectively (Table 4). However, the true test for this prediction approach would be its application to novel compounds. We have recently applied the average empirical scaling factors derived in this study for the seven literature compounds for simulation of the human PK of four novel OATP substrates entering a first in human study at Pfizer. The PBPK prediction methodology resulted in better predictions accuracy when compared to other allometric scaling and more traditional *in vitro* scaling

approaches (data not shown). In our study, we used the observed renal CL values determined from the clinical data. However, when conducting simulations for novel compounds, this parameter would need to be predicted from preclinical data.

In summary, this study has provided a systematic analysis of seven transporter substrates in SCHH. A mechanistic prediction methodology has been proposed for scaling of human PK for the compounds investigated using data generated in SCHH. Although this approach relies on the use of empirical scaling factors for active uptake and billiary efflux, it allows simultaneous assessment of multiple processes occurring in the hepatocytes in a mechanistic manner and improves our understanding of the relevance of these processes for hepatic disposition of drugs. The necessity for these empirical scaling factors needs to be further understood to increase confidence in the applicability of this methodology to novel compounds.

Acknowledgements

The assistance of scientists at the Hamner Institutes for Health Sciences (Research Triangle Park, NC), including Jerry Campbell and Alina Efremenko, in converting the code to acslX software and carrying out initial local sensitivity analyses is greatly appreciated.

DMD Fast Forward. Published on February 16, 2012 as DOI: 10.1124/dmd.111.042994
This article has not been copyedited and formatted. The final version may differ from this version.

Authorship Contribution

Participated in research design: Jones, Barton, Lai, El-Kattan, Fenner.

Conducted experiments: Lai, Bi, Kimoto, Kempshall, Tate, Fenner.

Contributed new reagents or analytical tools: Not Applicable.

Performed data analysis: Jones, Barton, Tate.

Wrote or contributed to writing the manuscript: Jones, Barton, Lai, Bi, Kimoto, Kempshall, Tate, El-Kattan, Houston, Galetin, Fenner.

DMD Fast Forward. Published on February 16, 2012 as DOI: 10.1124/dmd.111.042994
This article has not been copyedited and formatted. The final version may differ from this version.

References

Allan G, Davis J, Dickins M, Gardner I, Jenkins T, Jones H, Webster R, and Westgate H (2008) Pre-clinical pharmacokinetics of UK-453,061, a novel non-nucleoside reverse transcriptase inhibitor (NNRTI), and use of in silico physiologically based prediction tools to predict the oral pharmacokinetics of UK-453,061 in man. *Xenobiotica* 38:620-640.

Bergman E, Forsell P, Tevell A, Persson EM, Hedeland M, Bondesson U, Knutson L, and Lennernas H (2006) Biliary secretion of rosuvastatin and bile acids in humans during the absorption phase. *Eur J Pharm Sci* 29:205-214.

Bi YA, Kazolias D, and Duignan DB (2006) Use of cryopreserved human hepatocytes in sandwich culture to measure hepatobiliary transport. *Drug Metab Dispos* 34:1658-1665.

Bischoff KB (1975) Some fundamental considerations of the applications of pharmacokinetics to cancer chemotherapy. *Cancer Chemother Rep* 59:777-793.

De Buck SS, Sinha VK, Fenu LA, Nijsen MJ, Mackie CE, and Gilissen RA (2007) Prediction of human pharmacokinetics using physiologically based modeling: a retrospective analysis of 26 clinically tested drugs. *Drug Metab Dispos* 35:1766-1780.

Gertz M, Harrison A, Houston JB, and Galetin A (2010) Prediction of human intestinal first-pass metabolism of 25 CYP3A substrates from in vitro clearance and permeability data. *Drug Metab Dispos* 38:1147-1158.

Gertz M, Houston JB, and Galetin A (2011) Physiologically Based Pharmacokinetic Modeling of Intestinal First-Pass Metabolism of CYP3A Substrates with High Intestinal Extraction. *Drug Metab Dispos* 39:1633-1642.

Giacomini KM, Huang SM, Tweedie DJ, Benet LZ, Brouwer KL, Chu X, Dahlin A, Evers R, Fischer V, Hillgren KM, Hoffmaster KA, Ishikawa T, Keppler D, Kim RB, Lee CA, Niemi M, Polli JW, Sugiyama Y, Swaan PW, Ware JA, Wright SH, Yee SW, Zamek-Gliszczynski MJ, and Zhang L (2010) Membrane transporters in drug development. *Nat Rev Drug Discov* 9:215-236.

Hilgendorf C, Ahlin G, Seithel A, Artursson P, Ungell AL, and Karlsson J (2007) Expression of thirty-six drug transporter genes in human intestine, liver, kidney, and organotypic cell lines. *Drug Metab Dispos* 35:1333-1340.

Houston JB (1994) Utility of in vitro drug metabolism data in predicting in vivo metabolic clearance. *Biochem Pharmacol* 47:1469-1479.

Jones HM, Gardner IB, Collard WT, Stanley PJ, Oxley P, Hosea NA, Plowchalk D, Gernhardt S, Lin J, Dickins M, Rahavendran SR, Jones BC, Watson KJ, Pertinez H, Kumar V, and Cole S (2011) Simulation of human intravenous and oral pharmacokinetics of 21 diverse compounds using physiologically based pharmacokinetic modelling. *Clin Pharmacokinet* 50:331-347.

Jones HM, Parrott N, Jorga K, and Lave T (2006) A novel strategy for physiologically based predictions of human pharmacokinetics. *Clin Pharmacokinet* 45:511-542.

Kawai R, Mathew D, Tanaka C, and Rowland M (1998) Physiologically based pharmacokinetics of cyclosporine A: extension to tissue distribution kinetics in rats and scale-up to human. *J Pharmacol Exp Ther* 287:457-468.

Kitamura S, Maeda K, Wang Y, and Sugiyama Y (2008) Involvement of multiple transporters in the hepatobiliary transport of rosuvastatin. *Drug Metab Dispos* 36:2014-2023.

Kotani N, Maeda K, Watanabe T, Hiramatsu M, Gong LK, Bi YA, Takezawa T, Kusuhara H, and Sugiyama Y (2011) Culture period-dependent changes in the uptake of transporter substrates in sandwich-cultured rat and human hepatocytes. *Drug Metab Dispos* 39:1503-1510.

Lave T, Coassolo P, Ubeaud G, Brandt R, Schmitt C, Dupin S, Jaeck D, and Chou RC (1996) Interspecies scaling of bosentan, a new endothelin receptor antagonist and integration of in vitro data into allometric scaling. *Pharm Res* 13:97-101.

Lee JK, Marion TL, Abe K, Lim C, Pollock GM, and Brouwer KL (2010) Hepatobiliary disposition of troglitazone and metabolites in rat and human sandwich-cultured hepatocytes: use of Monte Carlo simulations to assess the impact of changes in biliary excretion on troglitazone sulfate accumulation. *J Pharmacol Exp Ther* 332:26-34.

Li N, Singh P, Mandrell KM, and Lai Y (2010) Improved extrapolation of hepatobiliary clearance from in vitro sandwich cultured rat hepatocytes through absolute quantification of hepatobiliary transporters. *Mol Pharm* 7:630-641.

Liu X, LeCluyse EL, Brouwer KR, Lightfoot RM, Lee JI, and Brouwer KL (1999) Use of Ca2+ modulation to evaluate biliary excretion in sandwich-cultured rat hepatocytes. *J Pharmacol Exp Ther* 289:1592-1599.

Liu L, Pang KS (2006) An integrated approach to model hepatic drug clearance. *Eur J Pharm Sci*. 29:215-30.

Mahagita C, Grassl SM, Piyachaturawat P, and Ballatori N (2007) Human organic anion transporter 1B1 and 1B3 function as bidirectional carriers and do not mediate GSH-bile acid cotransport. *Am J Physiol Gastrointest Liver Physiol* 293:G271-278.

Nezasa K, Takao A, Kimura K, Takaichi M, Inazawa K, and Koike M (2002) Pharmacokinetics and disposition of rosuvastatin, a new 3-hydroxy-3-methylglutaryl coenzyme A reductase inhibitor, in rat. *Xenobiotica* 32:715-727.

Paine SW, Parker AJ, Gardiner P, Webborn PJ, and Riley RJ (2008) Prediction of the pharmacokinetics of atorvastatin, cerivastatin, and indomethacin using kinetic models applied to isolated rat hepatocytes. *Drug Metab Dispos* 36:1365-1374.

Poirier A, Cascais AC, Funk C, and Lave T (2009a) Prediction of pharmacokinetic profile of valsartan in human based on in vitro uptake transport data. *J Pharmacokinet Pharmacodyn* 36:585-611.

Poirier A, Funk C, Scherrmann JM, and Lave T (2009b) Mechanistic modeling of hepatic transport from cells to whole body: application to napsagatran and fexofenadine. *Mol Pharm* 6:1716-1733.

Poirier A, Lave T, Portmann R, Brun ME, Senner F, Kansy M, Grimm HP, and Funk C (2008) Design, data analysis, and simulation of in vitro drug transport kinetic experiments using a mechanistic in vitro model. *Drug Metab Dispos* 36:2434-2444.

Poulin P and Theil FP (2000) A priori prediction of tissue:plasma partition coefficients of drugs to facilitate the use of physiologically-based pharmacokinetic models in drug discovery. *J Pharm Sci* 89:16-35.

Reinoso RF, Telfer BA, Brennan BS, and Rowland M (2001) Uptake of teicoplanin by isolated rat hepatocytes: comparison with in vivo hepatic distribution. *Drug Metab Dispos* 29:453-459.

Rodgers T and Rowland M (2006) Physiologically based pharmacokinetic modelling 2: predicting the tissue distribution of acids, very weak bases, neutrals and zwitterions. *J Pharm Sci* 95:1238-1257.

Rostami-Hodjegan A and Tucker GT (2007) Simulation and prediction of in vivo drug metabolism in human populations from in vitro data. *Nat Rev Drug Discov* 6:140-148.

Schaefer O, Ohtsuki S, Kawakami H, Inoue T, Liehner S, Saito A, Sakamoto A, Ishiguro N, Matsumaru T, Terasaki T, and Ebner T (2011) Absolute Quantitation and Differential Expression of Drug Transporters, Cytochrome P450 Enzymes and UDP-Glucuronosyltransferases in Cultured Primary Human Hepatocytes. *Drug Metab Dispos*.

Soars MG, Webborn PJ, and Riley RJ (2009) Impact of hepatic uptake transporters on pharmacokinetics and drug-drug interactions: use of assays and models for decision making in the pharmaceutical industry. *Mol Pharm* 6:1662-1677.

Vavricka SR, Van Montfoort J, Ha HR, Meier PJ, and Fattinger K (2002) Interactions of rifamycin SV and rifampicin with organic anion uptake systems of human liver. *Hepatology* 36:164-172.

Watanabe T, Kusuhara H, Maeda K, Kanamaru H, Saito Y, Hu Z, and Sugiyama Y (2010) Investigation of the rate-determining process in the hepatic elimination of HMG-CoA reductase inhibitors in rats and humans. *Drug Metab Dispos* 38:215-222.

Watanabe T, Kusuhara H, Maeda K, Shitara Y, and Sugiyama Y (2009) Physiologically based pharmacokinetic modeling to predict transporter-mediated clearance and distribution of pravastatin in humans. *J Pharmacol Exp Ther* 328:652-662.

Wu CY and Benet LZ (2005) Predicting drug disposition via application of BCS: transport/absorption/ elimination interplay and development of a biopharmaceutics drug disposition classification system. *Pharm Res* 22:11-23.

Yabe Y, Galetin A, and Houston JB (2011) Kinetic characterization of Rat Hepatic Uptake of 16 Actively Transported Drugs. *Drug Metab Dispos*.

Yamashiro W, Maeda K, Hirouchi M, Adachi Y, Hu Z, and Sugiyama Y (2006) Involvement of transporters in the hepatic uptake and biliary excretion of valsartan, a selective antagonist of the angiotensin II AT1-receptor, in humans. *Drug Metab Dispos* 34:1247-1254.

Yan GZ, Brouwer KL, Pollack GM, Wang MZ, Tidwell RR, Hall JE, and Paine MF (2011) Mechanisms underlying differences in systemic exposure of structurally similar active metabolites: comparison of two preclinical hepatic models. *J Pharmacol Exp Ther* 337:503-512.

Footnotes

Financial Disclosure: H.M.J., S.K., K.S.F., H.B., Y.L., Y.B., E.K. and A.E-K. were all employees of Pfizer during this research.

DMD Fast Forward. Published on February 16, 2012 as DOI: 10.1124/dmd.111.042994
This article has not been copyedited and formatted. The final version may differ from this version.

Figure Legends

Figure 1 – Schematic of the *in vitro* model (A) Conditions: 0.1mM Rifamycin SV; (B) Conditions: HBSS; (C) Conditions Ca^{2+}/Mg^{2+} free, 1mM EGTA

Figure 2 – Schematic of the *in vivo* PBPK model

Figure 3 – Simulated, fitted and observed human i.v. plasma concentration-time profiles for (A) pravastatin; (B) cerivastatin; (C) bosentan; (D) fluvastatin; (E) rosuvastatin; (F) valsartan and (G) repaglinide

open squares represent observed data; solid line represents predicted data using the PBPK model; dashed line represents fitted data

Figure 4 – Simulated (using the average empirical scaling factor for individual processes) and observed human i.v. plasma concentration-time profiles for (A) pravastatin; (B) cerivastatin; (C) bosentan; (D) fluvastatin; (E) rosuvastatin; (F) valsartan and (G) repaglinide

open squares represent observed data; solid line represents predicted data using the PBPK model and the average empirical scaling factors listed in Table 3

Figure 5 – Time dependent sensitivity analysis of the importance of CLint,u,act, CLint,u,pass, CLint,u,met and CLint,u,bile parameters on the plasma kinetics of

(A) pravastatin; (B) cerivastatin; (C) bosentan; (D) fluvastatin; (E) rosuvastatin; (F) valsartan and (G) repaglinide

DMD Fast Forward. Published on February 16, 2012 as DOI: 10.1124/dmd.111.042994
This article has not been copyedited and formatted. The final version may differ from this version.

solid line represents CLint,u,act; dashed line represents CLint,u,pass; dotted line represents CLint,u,met; dash-dot line represents CLint,u,bile and dash-dot-dot line represents renal CL

Table 1 – Physicochemical, *in vitro* and clinical pharmacokinetic properties for the compounds studied

Compound	LogD $_{7.4}$	Charge[1]	pKa	B:P ratio	fu,p	HLM CLint,u,met µl/min/mg
Pravastatin	-0.84	A	4.6	0.55	0.43	0
Cerivastatin	1.8	Z	5.3(B); 5.0(A)	0.76	0.0048	29
Bosentan	1.3	A	5.2	0.48	0.0053	22[2]
Fluvastatin	1.6	A	4.6	0.57	0.0041	76
Rosuvastatin	-0.33	A	4.2	0.56	0.094	0
Valsartan	-0.88	A	3.8; 4.6	0.55	0.0010	0
Repaglinide	2.1	Z	6.1(B); 4.4(A)	0.48	0.0074	128[3]

[1] A=acidic, B=basic, Z=zwitterionic; [2] (Lave et al., 1996), corrected for microsomal binding (fu = 0.87); [3] (Gertz et al., 2010)

Table 2 – *In vitro* parameters estimated from sandwich culture human hepatocyte parameters at a single substrate concentration. Data represent mean from multiple replicates in 1-2 donors (standard deviation; where replicates are >2)

Compound[1]	CLint,u,active µl/min/Mcells	CLint,u,passive µl/min/Mcells	CLint,u,bile µl/min/Mcells	Predicted fu,cell
Pravastatin	1.8	0.1	1.2	0.60
Cerivastatin	9.6 (2.7)	25 (3.5)	6.2 (1.8)	0.0096
Bosentan	9.1	4.8	7.4	0.011
Fluvastatin	45 (21)	20 (9.6)	17	0.0082
Rosuvastatin	9.3 (2.6)	1.7 (0.73)	1.5 (0.088)	0.17
Valsartan	2.1 (0.48)	0.60 (0.18)	96	0.0020
Repaglinide	30 (16)	89 (75)	0	0.015

[1]Lots: Pravastatin: BD109 (n=1), HU4168 (n=1); Cerivastatin: BD109 (n=2), HU4168 (n=2); Bosentan: HU4168 (n=1); Fluvastatin: BD109 (n=2), HU4168 (n=1); Rosuvastatin: BD109 (n=6), HU4166 (n=2); Valsartan: BD109 (n=2), HU4168 (n=1); Repaglinide: HU4168 (n=3), RTM (n=2)

Table 3 – *In vitro* scaled and fitted sandwich culture human hepatocyte estimates

Compound	SCLint,u,act L/hr			SCLint,u,pass L/hr			SCLint,u,bile L/hr		
	In vitro scaled	*In vivo* fitted	Scaling factor	*In vitro* scaled	*In vivo* fitted	Scaling factor	*In vitro* scaled	*In vivo* fitted	Scaling factor
Pravastatin	19	406	21	1.1	4.2	3.9	12	1.5	0.12
Cerivastatin	102	12827	126	265	153	0.58	182[1]	55[1]	-
Bosentan	96	8489	89	51	59	1.2	165[1]	21[1]	-
Fluvastatin	475	76513	161	208	147	0.71	485[1]	86[1]	-
Rosuvastatin	98	1190	12	18	1.7	0.10	16	1.2	0.079
Valsartan	22	2463	110	6.4	23	3.7	1017	25	0.024
Repaglinide	319	13941	44	938	1477	1.6	0	0	-
Geometric mean	-	-	58	-	-	1.0	-	-	0.061

[1]repesents the sum of SCLint,u, bile and SCLint,u,met as for these 3 compounds both CL mechanisms are occurring and they cannot be uniquely identified in the fitting process

Table 4 – Predicted CL and Vss parameters for the seven drugs investigated using different modeling scenarios

Compound	CL mL/min/kg			Vss L/Kg		
	Clinical[1]	*In vitro* scaled[2]	*In vitro* scaled + Scaling factor	Clinical[1]	*In vitro* scaled[2]	*In vitro* scaled + Scaling factor
Pravastatin	14	8.0	17	0.46	0.20	0.36
Cerivastatin	2.9	0.17	2.0	0.33	0.15	0.21
Bosentan	2.3	0.14	3.5	0.67	0.12	0.17
Fluvastatin	8.7	0.46	8.1	0.16	0.13	0.16
Rosuvastatin	11	4.0	7.6	1.7	0.15	1.5
Valsartan	0.49	0.15	0.42	0.23	0.11	0.12
Repaglinide	7.8	0.74	6.4	0.35	0.15	0.16
Absolute average fold error	-	7.1	1.3	-	3.0	1.7

[1] reported i.v. CL and Vss parameters from publications reported in Supplementary Material, Table S1; [2] predicted i.v. CL and Vss parameters determined by non-compartmental analysis of predicted profiles.

FIGURE 1

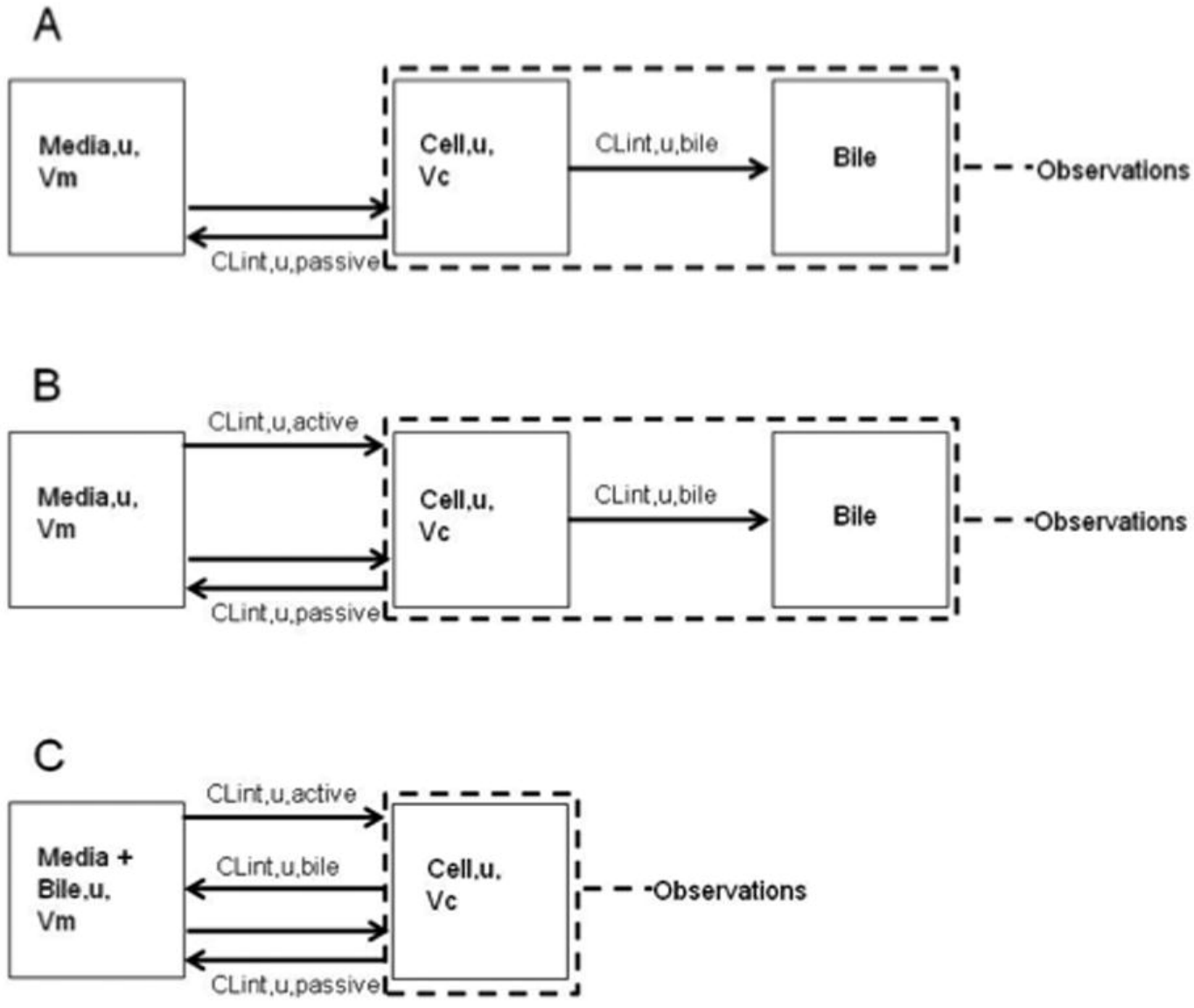
A
Media,u,
Vm
Cell,u,
Vc
CLint,u,bile
Bile
Observations
CLint,u,passive
B
CLint,u,active
Media,u,
Vm
Cell,u,
Vc
CLint,u,bile
Bile
Observations
CLint,u,passive
C
CLint,u,active
Media +
Bile,u,
Vm
CLint,u,bile
Cell,u,
Vc
Observations
CLint,u,passive

FIGURE 2

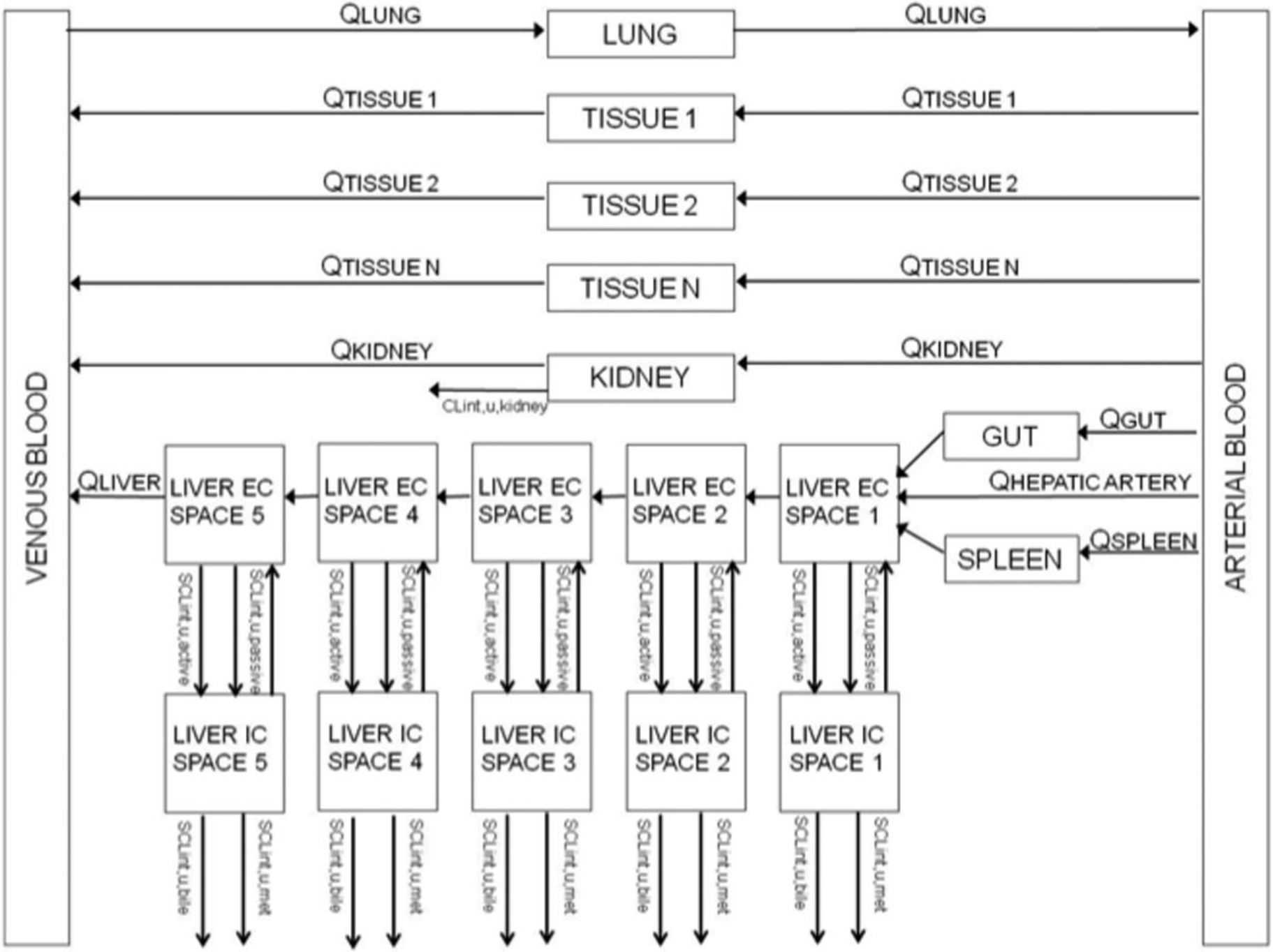
VENOUS BLOOD
ARTERIAL BLOOD
QLUNG
LUNG
QLUNG
QTISSUE 1
TISSUE 1
QTISSUE 1
QTISSUE 2
TISSUE 2
QTISSUE 2
QTISSUE N
TISSUE N
QTISSUE N
QKIDNEY
KIDNEY
QKIDNEY
CLint,u,kidney
GUT
QGUT
QHEPATIC ARTERY
SPLEEN
QSPLEEN
QLIVER
LIVER EC SPACE 5
LIVER EC SPACE 4
LIVER EC SPACE 3
LIVER EC SPACE 2
LIVER EC SPACE 1
SCLint,u,active
SCLint,u,passive
LIVER IC SPACE 5
LIVER IC SPACE 4
LIVER IC SPACE 3
LIVER IC SPACE 2
LIVER IC SPACE 1
SCLint,u,bile
SCLint,u,met

FIGURE 3

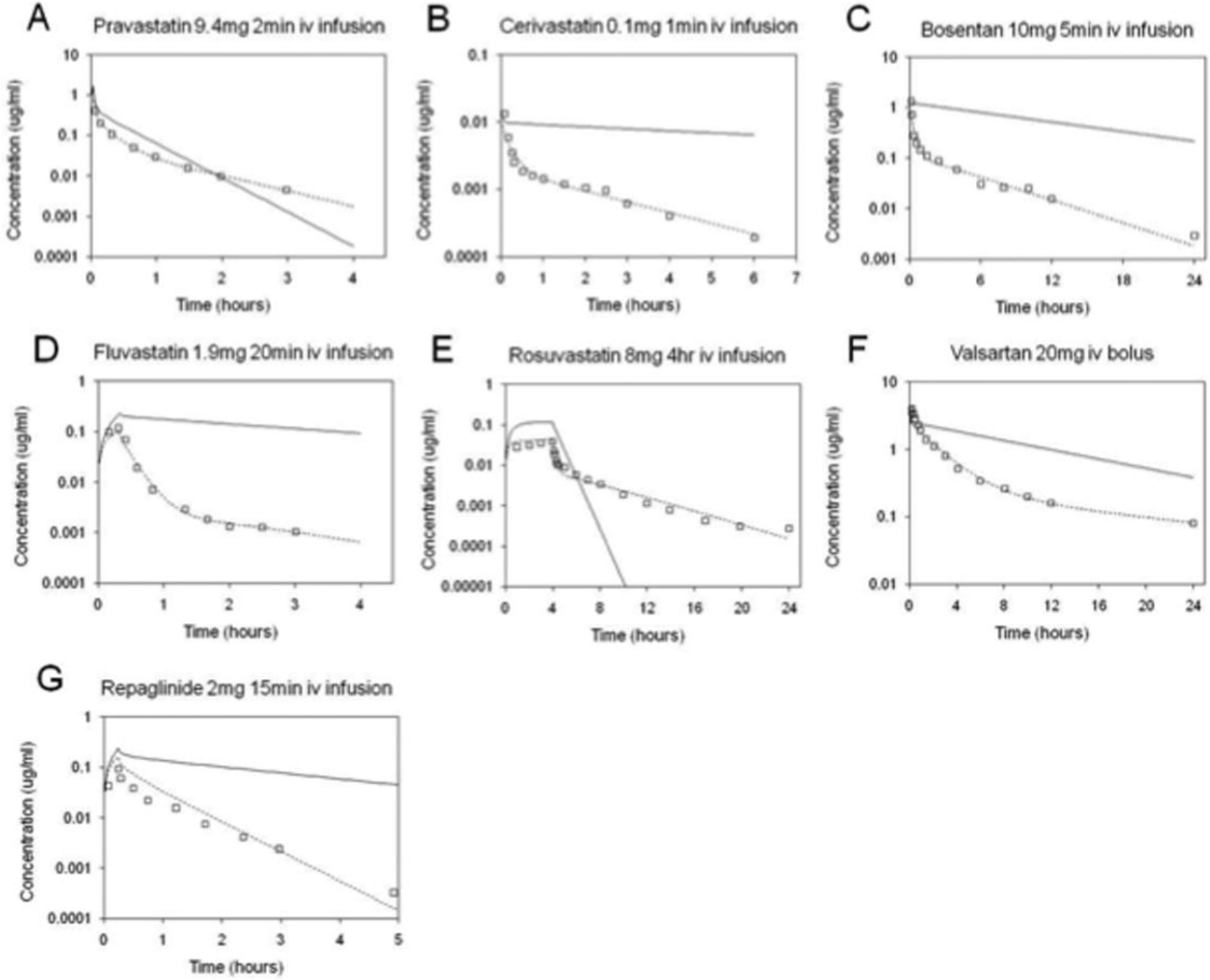
A
Pravastatin 9.4mg 2min iv infusion
Concentration (ug/ml)
Time (hours)
B
Cerivastatin 0.1mg 1min iv infusion
Concentration (ug/ml)
Time (hours)
C
Bosentan 10mg 5min iv infusion
Concentration (ug/ml)
Time (hours)
D
Fluvastatin 1.9mg 20min iv infusion
Concentration (ug/ml)
Time (hours)
E
Rosuvastatin 8mg 4hr iv infusion
Concentration (ug/ml)
Time (hours)
F
Valsartan 20mg iv bolus
Concentration (ug/ml)
Time (hours)
G
Repaglinide 2mg 15min iv infusion
Concentration (ug/ml)
Time (hours)

FIGURE 4

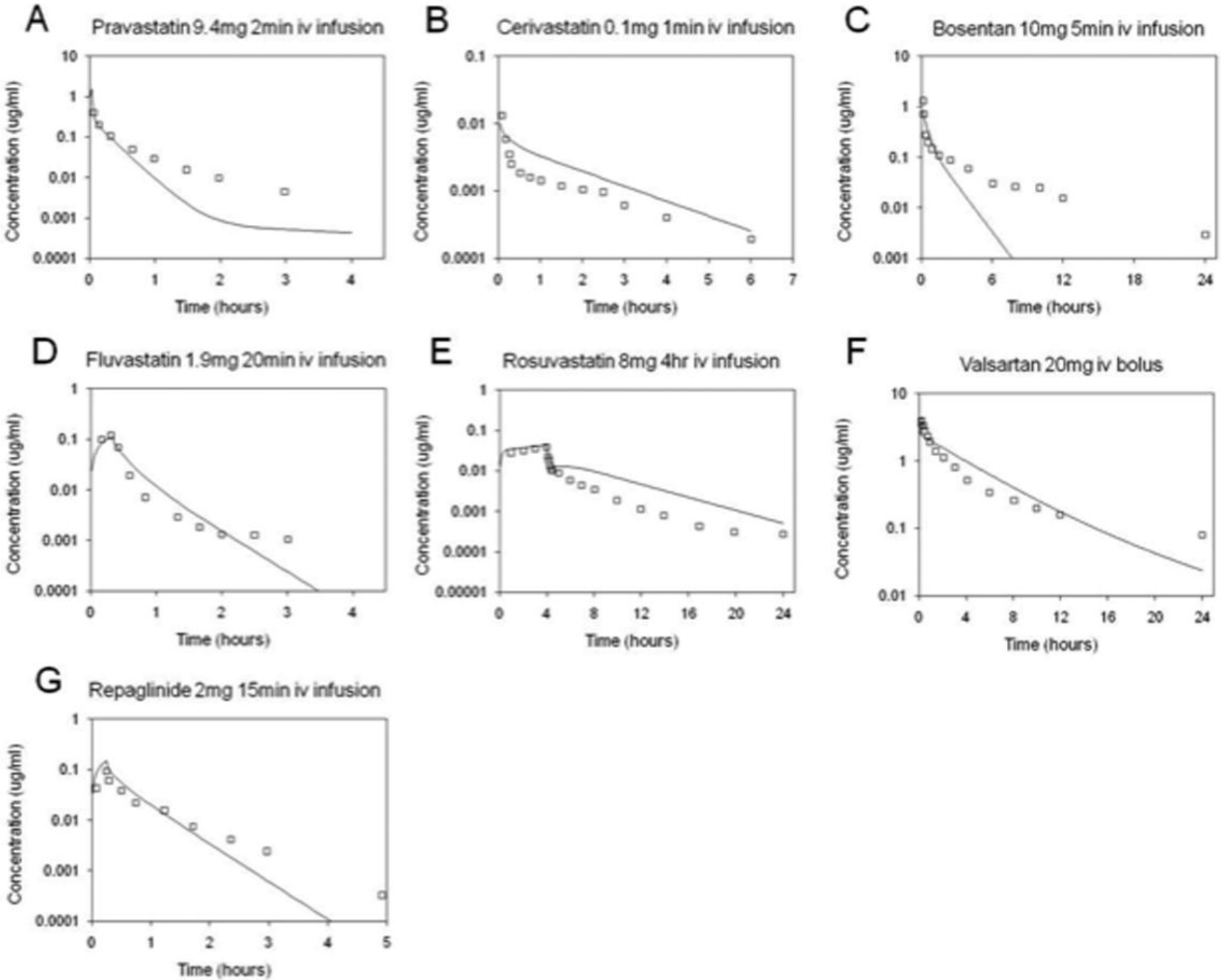
A
Pravastatin 9.4mg 2min iv infusion
B
Cerivastatin 0.1mg 1min iv infusion
C
Bosentan 10mg 5min iv infusion
D
Fluvastatin 1.9mg 20min iv infusion
E
Rosuvastatin 8mg 4hr iv infusion
F
Valsartan 20mg iv bolus
G
Repaglinide 2mg 15min iv infusion
Concentration (ug/ml)
Time (hours)

FIGURE 5

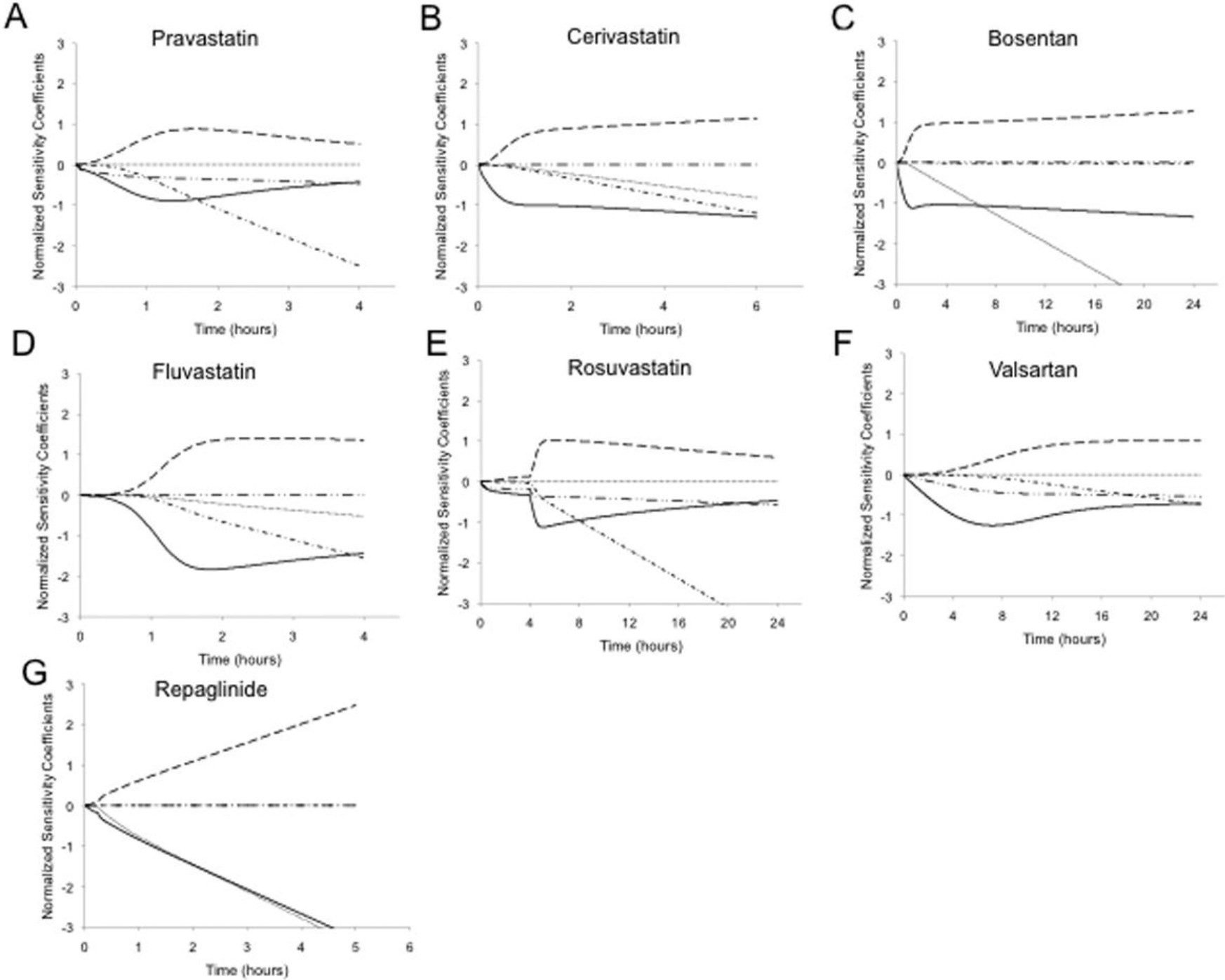
A
Pravastatin
B
Cerivastatin
C
Bosentan
D
Fluvastatin
E
Rosuvastatin
F
Valsartan
G
Repaglinide
Normalized Sensitivity Coefficients
Time (hours)

Supplementary Material

Journal:

Drug Metabolism and Disposition

Title of Article:

Mechanistic pharmacokinetic modeling for the prediction of transporter-mediated disposition in human from sandwich culture human hepatocyte data

Author's names:

Hannah M Jones, Hugh A Barton, Yurong Lai, Yi-an Bi, Emi Kimoto, Sarah Kempshall, Sonya C Tate, Ayman El-Kattan, J Brian Houston, Aleksandra Galetin and Katherine S Fenner

Figure S1: Raw SCHH data for (A-B) pravastatin, (C-F) cerivastatin, (G) bosentan, (H-J) fluvastatin, (K-R) rosuvastatin, (S-U) valsartan and (V-X) repaglinide.

Solid diamonds represent HBSS only, open squares represent Ca2+/Mg2+ free, solid triangles represent HBSS + Rifamycin SV

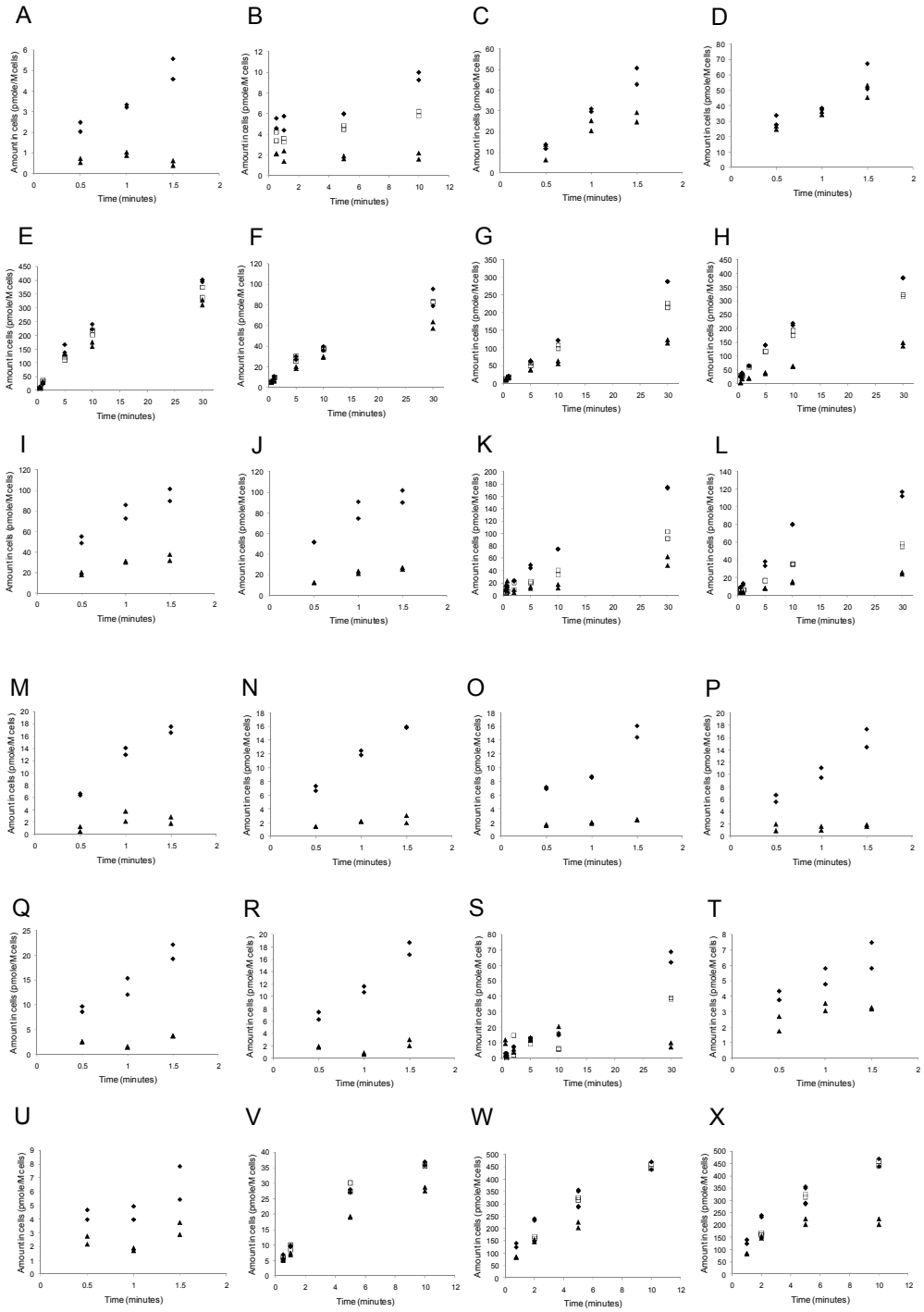

Figure S2: Fitted versus observed human plasma concentration time data for (A) pravastatin, (B) cerivastatin, (C) bosentan, (D) fluvastatin, (E) rosuvastatin, (F) valsartan, (G) repaglinide.

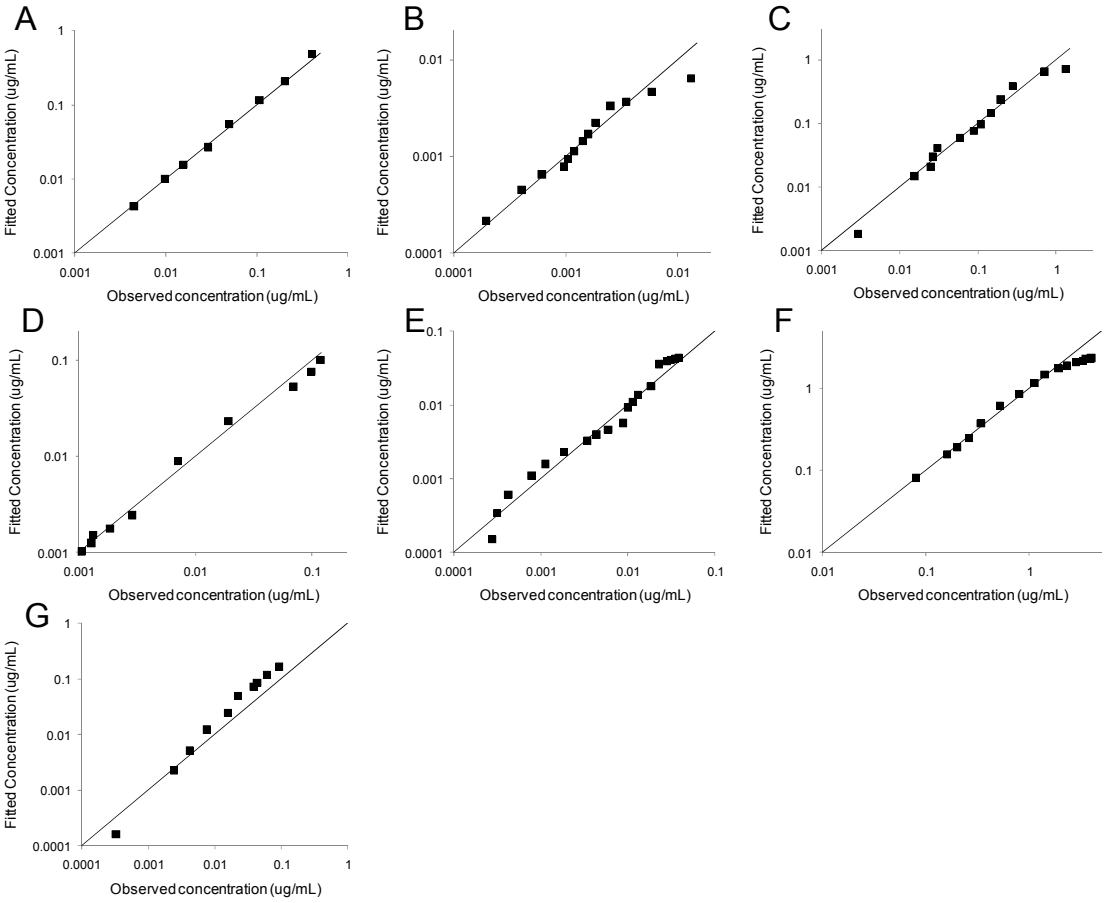

Figure S3: Contour plots for pairs of fitted parameters (A-C) pravastatin, (D-F) cerivastatin, (G-I) bosentan, (J-L) fluvastatin, (M-O) rosuvastatin, (P-R) valsartan and (S) repaglinide.

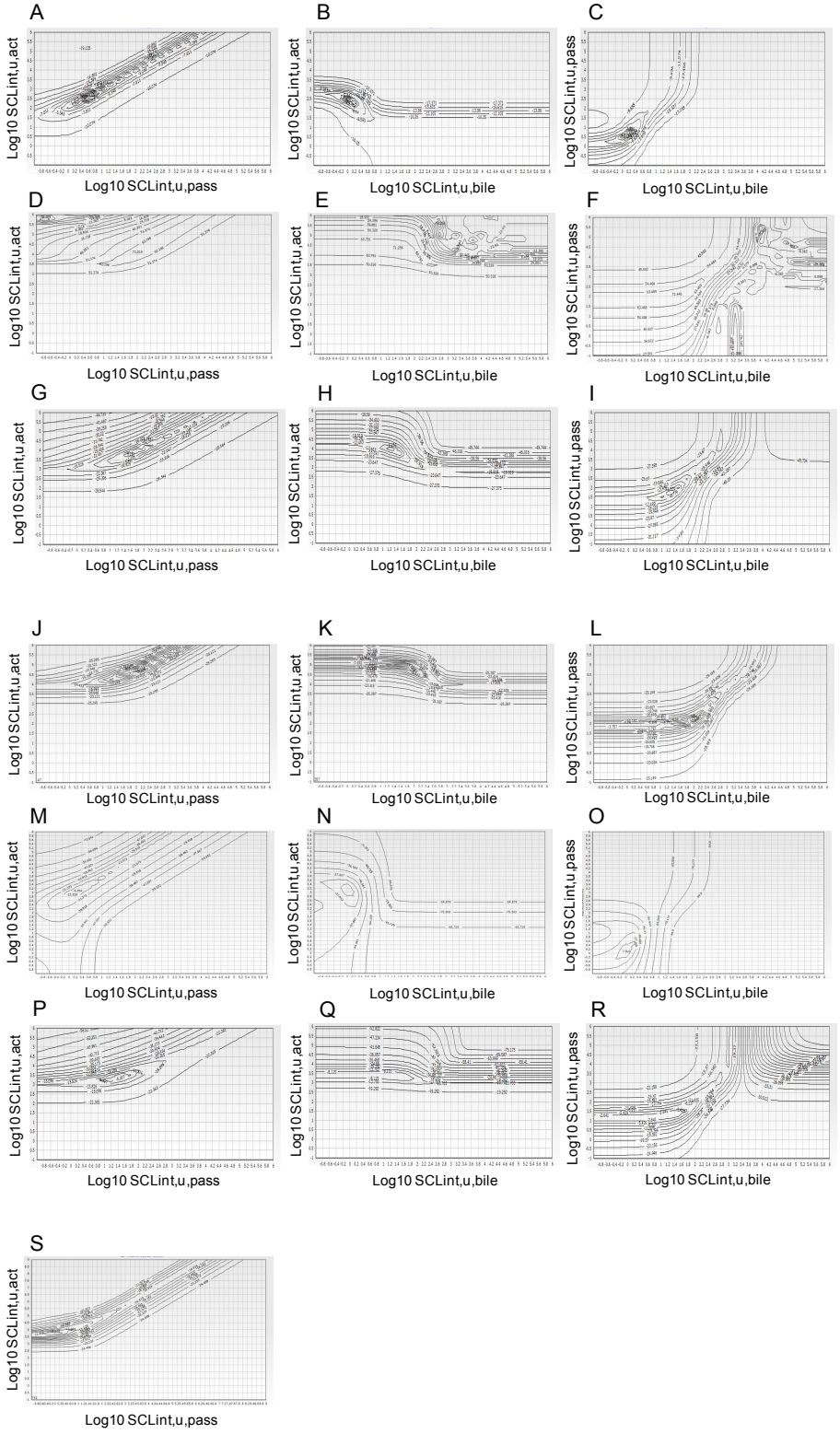

Table S1 – Clinical pharmacokinetic properties and substrate specificity for the compounds studied

Compound	CL,i.v. mL/min/kg	Vss,i.v. L/Kg	% renal CL	Substrate specificity
Pravastatin[1]	14	0.46	47	OATP1B1, MRP2
Cerivastatin[2]	2.9	0.33	0	OATP1B1, CYP3A4, 2C8
Bosentan[3]	2.3	0.67	0	OATP1B1, 1B3, 2B1, CYP3A4, 2C9
Fluvastatin[4]	8.7	0.16	0	OATP1B1, 2B1, 1B3, CYP2C9
Rosuvastatin[5]	11	1.7	30	OATP1B1, 1B3, 2B1, BCRP
Valsartan[6]	0.49	0.23	29	OATP1B1, 1B3
Repaglinide[7]	7.8	0.35	0	OATP1B1, CYP3A4, 2C8

[1] Singhvi et al., 1990; [2] Muck et al., 1997; [3] Weber et al., 1996; [4]Lindahl et al., 1996; [5]Martin et al., 2003; [6]Flesch et al., 1997; [7] Hatorp et al., 1998

Table S2 Quantification of OATP1B1, 1B3 and 2B1 in suspension hepatocytes and SCHH

	Suspension	SCHH at day 5	Change compared to suspension
	(fmol/ug protein)		%
OATP1B1	3.42±0.11	5.28±0.22	154[1]
OATP1B3	1.50±0.15	0.88±0.11	59[1]
OATP2B1	1.84±0.15	1.23±0.12	67*

[1] P<0.05, as compared to suspension.

Supplementary References

Flesch G, Muller P, and Lloyd P (1997) Absolute bioavailability and pharmacokinetics of valsartan, an angiotensin II receptor antagonist, in man. *Eur J Clin Pharmacol* 52:115-120.

Hatorp V, Oliver S, and Su CA (1998) Bioavailability of repaglinide, a novel antidiabetic agent, administered orally in tablet or solution form or intravenously in healthy male volunteers. *Int J Clin Pharmacol Ther* 36:636-641.

Lindahl A, Sandstrom R, Ungell AL, Abrahamsson B, Knutson TW, Knutson L, and Lennernas H (1996) Jejunal permeability and hepatic extraction of fluvastatin in humans. *Clin Pharmacol Ther* 60:493-503.

Martin PD, Warwick MJ, Dane AL, Brindley C, and Short T (2003) Absolute oral bioavailability of rosuvastatin in healthy white adult male volunteers. *Clin Ther* 25:2553-2563.

Muck W, Ritter W, Ochmann K, Unger S, Ahr G, Wingender W, and Kuhlmann J (1997) Absolute and relative bioavailability of the HMG-CoA reductase inhibitor cerivastatin. *Int J Clin Pharmacol Ther* 35:255-260.

Singhvi SM, Pan HY, Morrison RA, and Willard DA (1990) Disposition of pravastatin sodium, a tissue-selective HMG-CoA reductase inhibitor, in healthy subjects. *Br J Clin Pharmacol* 29:239-243.

Weber C, Schmitt R, Birnboeck H, Hopfgartner G, van Marle SP, Peeters PA, Jonkman JH, and Jones CR (1996) Pharmacokinetics and pharmacodynamics of the endothelin-receptor antagonist bosentan in healthy human subjects. *Clin Pharmacol Ther* 60:124-137.